

DTIC FILE COPY

(2)

AD-A219 620

FRACTAL TERRAIN ANALYSIS FROM AN ATTRACTOR VIEWPOINT

FINAL REPORT

M. ANN PIECH

February 26, 1990

DTIC
ELECTE
MAR 07 1990
S D CS D

U. S. ARMY RESEARCH OFFICE

DAAL03-86-K-0141

STATE UNIVERSITY OF NEW YORK AT BUFFALO

APPROVED FOR PUBLIC RELEASE;
DISTRIBUTION UNLIMITED

50 08 05 3

Table of Contents

Project Objective	1
Scale Space and Fingerprint Background	1
Summary of Program Results	5
Publications	13
Abstracts of Publications	14
Participating Scientific Personnel	16
DD Form 1473	17

Accession For	
NTIS CRA&I	<input checked="checked" type="checkbox"/>
DTIC TAB	<input type="checkbox"/>
Unannounced	<input type="checkbox"/>
Justification	
By	
Date	
Approved by	
Signature	
A-1	

I. Project Objective

The objective of this program was to develop a new approach to modeling terrain using mathematical concepts from fractal and attractor theories. Key parameters of the model were extracted from fingerprint analysis based on scale space smoothings of elevation profiles.

II. Scale Space and Fingerprint Background

Description of terrain involves identification, over a broad range of physical scales, of the spatial extent, prevalence, and relative importance of elements such as peaks, ridges, and valleys. These elements are delimited by fundamental edges of the topography, and so it is natural to propose terrain modeling based on a scale space filtering of elevation data. A scale space image is a set of progressively smoothed versions of the original topographic array; as the smoothing scale increases, features of the terrain disappear until only a dominant terrain shape remains. A plot of the points of inflection, or edges, within the scale space image results in a 'fingerprint' of the terrain. The fingerprint locates points of inflection of the original data, provides a context in which the inflection points are paired and assigned to a topographic feature, and relates topographic features of the curve to each other.

Witkin developed the scale space fingerprint technique in order to relate signal descriptions across different filtering scales (Ref. 2). Its mathematical foundation lies in the theory of heat flow. A signal f (in our case f is a slice of a topographic elevation array) can be regarded as an initial temperature distribution on the real line. As heat flows, the temperature distribution smoothes; weak features (local hot or cold spots) vanish in a short time while stronger features persist for longer times. A feature is delimited by its left and right inflection points; when these points merge, the feature vanishes. No new features (sources or sinks) arise during heat flow. The complete temperature record is

called the scale space image, and the graph of inflection points over time is called the fingerprint. Scale space techniques have recently been applied to edge detection and pattern recognition, to the cartographic matching of shorelines, to histogram analysis of normal mixtures, and to modeling and analysis of hyperspectral data curves.

In applying scale space techniques to terrain analysis, the input signal $f(x)$ is an elevation profile obtained by either an east-west or a north-south scan from 7.5 minute United States Geological Survey Digital Elevation Model (DEM) records. One x-unit corresponds to 30 meters. G^σ is a mean zero Gaussian mask with standard deviation $\sigma > 0$:

$$G^\sigma(y) = \frac{1}{\sqrt{2\pi} \sigma} e^{-y^2/2\sigma^2}$$

When we convolve f with G^σ , we obtain the scale space image

$$F(x, \sigma) = (f * G^\sigma)(x) = \int_{-\infty}^{\infty} f(x-y) G^\sigma(y) dy$$

For each fixed σ , $F(x, \sigma)$ is a smoothing of $f(x)$. An edge occurs where a function is changing most rapidly. Equivalently, edges are points of inflection, where the slope has a local maximum or minimum. The fingerprint tracks the location of inflection points of $F(x, \sigma)$ against smoothing scale σ ; thus, it is the plot of all points (x, σ) where $F_{xx}(x, \sigma)$ changes sign (Fig. 1).

The input f of our terrain analysis consists of discrete elevation data, yet our scale space analysis involves differentiation to get slopes and inflection points. Gaussian convolution efficiently deals with this problem, since the result of convolution of a bounded measurable f with a smooth kernel such as the Gaussian produces an output function that inherits the differential properties of the kernel. In particular,

$$\frac{d}{dx} \int_{-\infty}^{\infty} f(y) G^\sigma(x-y) dy = \int_{-\infty}^{\infty} f(y) G_x^\sigma(x-y) dy$$

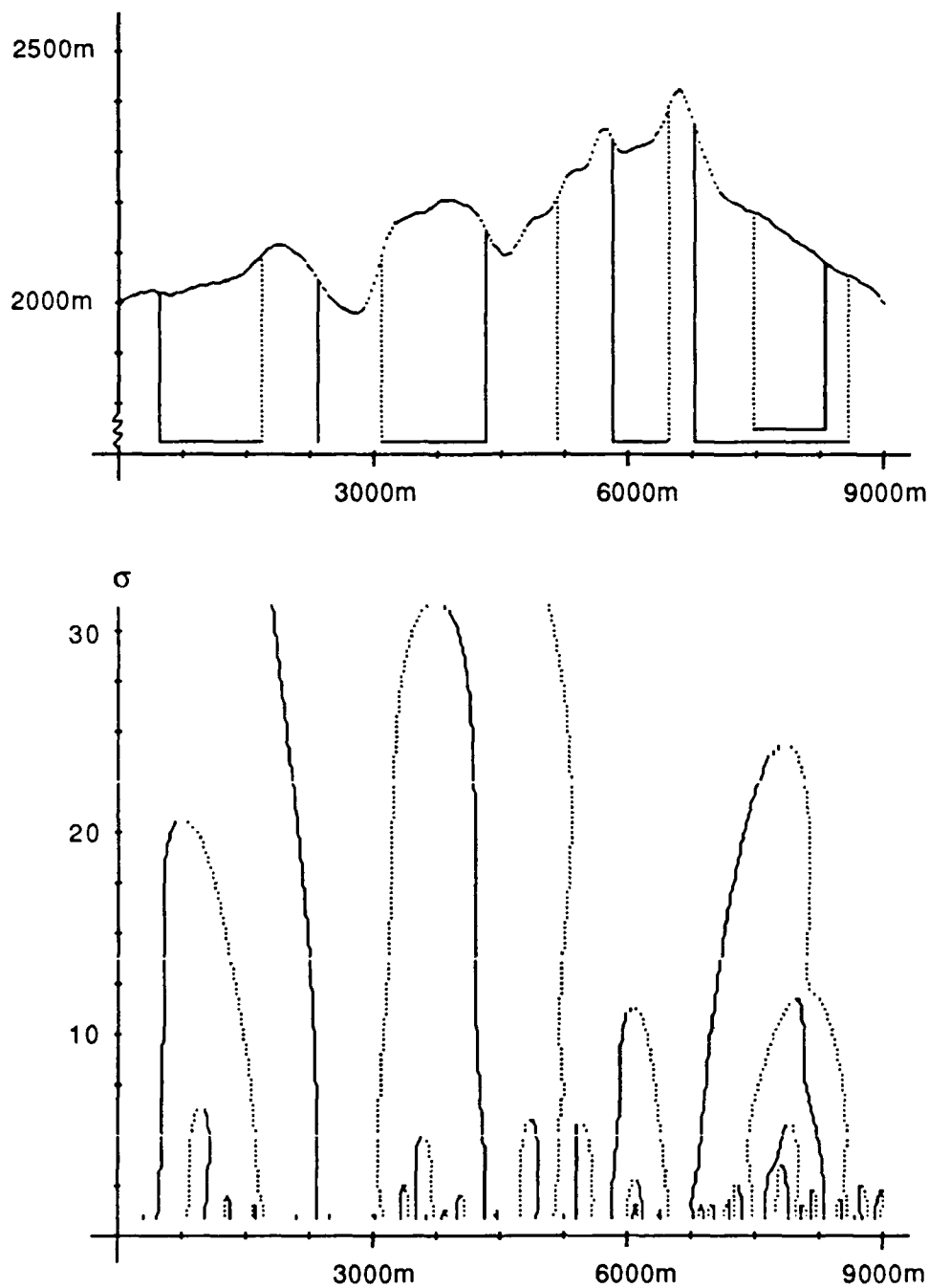


Fig. 1. An elevation profile (top) and corresponding fingerprint (bottom) for a 9,000 m trace from the Lassen Volcanic Wilderness region of California. Location of features with closing scale $\sigma \geq 7$ are superimposed on the elevation profile. Each unit of σ corresponds to a data spacing unit of 30 meters.

and if L is any linear differential operator, then

$$L(f \cdot G^\sigma) = f \cdot LG^\sigma$$

Since we use numerical convolution based at each data point, we are able to calculate derivatives at each data point. Gaussian convolution is particularly well suited to handling differentiation of discrete imagery, since in a single operation, such as $f \cdot (G^\sigma)'$, we both smooth and differentiate. The degree of smoothing, or filtering, is controlled by the standard deviation parameter σ of the Gaussian kernel.

The Gaussian G^σ shares a variation diminishing property with other diffusion kernels: the number of zero-crossings of $f \cdot G^\sigma$ is not more than the number of zero-crossings of f . Consequently, the number of inflection points of $F(x, \sigma)$ also cannot increase when σ increases. This last property imparts a characteristic appearance to a fingerprint. Qualitatively, a fingerprint appears as an assemblage of closed arches (Fig.1, Fig. 2). Each arch is composed of a pair of zero-crossing contours of $F_{xx}(x, \sigma)$, one solid (darker) contour and one dotted (lighter) contour. As we cross a solid contour from left to right, the smoothed curve $F(x, \sigma)$ changes from concave down to concave up. As we cross a dotted contour from left to right, $F(x, \sigma)$ changes from concave up to concave down. As the smoothing scale σ increases, zero crossing contours pair off, merge to form an arch, and die out at the apex of the arch. The variation diminishing property of G^σ ensures that new contours cannot appear at positive values of σ , nor can arches be closed from below.

A feature is delimited by right and left inflection points. Each closed arch of a fingerprint corresponds to a feature. For example, an arch composed of a dotted left contour and a solid right contour represents a hill. Often fingerprint arches are nested: a hillock within a valley would give rise to nested arches, the hillock corresponding to the inner, lower arch. The use of inflection points to delimit features seems more natural than using relative maxima or minima of elevation to delimit hills or valleys. At each smoothing scale σ , the inflection points of $F(x, \sigma)$ segment the x -axis into mutually disjoint hills or valleys. If, instead, we were to consider a hill as delimited by adjacent relative minima, and

a valley as delimited by adjacent relative maxima, then hills and valleys would contain substantial intervals of overlap.

Sign changes of the inflection points in the upper and lower parts of Fig. 1 have been encoded by solid and dotted lines. A closed arch formed by a solid-dotted line is a subtraction feature or dip, while a closed arch formed by a dotted-solid line pair is an addition feature, or local peak. Note how solid and dotted lines alternate at any given value of sigma. By reading the fingerprint from higher to lower values of sigma, we can describe the shape and properties of the elevation profile with an increasing level of detail. This qualitative description of the elevation profile from the fingerprint can be made much more quantitative; in fact, it is possible to reconstruct the entire elevation profile from the fingerprint to within a scaling parameter and a linear shift (Yuille and Poggio, Ref. 3). The fingerprint provides a method to identify and rank key features of an elevation profile and a formalism to describe a profile to arbitrary levels of detail.

III. Summary of Program Results

General properties of scale space analysis

Initial effort on this program focused on development of general properties of scale space analysis that are independent of application to particular forms of input data:

- (a) software development and testing
- (b) analysis of the influence on the fingerprint of software parameters, such as choice of data extension method, Gaussian mask size or mask cropping
- (c) formulation and testing of feature properties and relationships that can be deduced from the fingerprint.

Our scale space/fingerprint software was designed to handle very general input data, so that the analyses (b) and (c) were based on application of the software to a variety of input data, including synthetic curves representing common edge and feature types.

spectral reflectance curves of soils and common terrain materials, terrain elevation profiles, and spectroscopic data of various pathogenic and non-pathogenic chemicals. General scale space properties developed on this project are contained in publications [1, 2, 3], which we summarize individually. Abstracts of each of these papers are included in Section V of this report.

1. M. A. Piech and K. R. Piech. Symbolic representation of hyperspectral data. *Applied Optics* 26 (1987), 4018–4026.

The fingerprint provides a context within which inflection points are tracked across a continuous range of filtering scales. Lesser features die out before stronger ones. We can spatially locate a feature by the left and right locations of the base of its fingerprint arch. The scale at which an arch closes is a measure of the magnitude or persistence of the feature. This measure enables us to compare magnitudes of distant, as well as near, features. Each feature can be described by a triplet consisting of the scale at which the feature arch closes, and the left and right inflection points delimiting the feature. This description is compact, quantitative and hierarchical, describing the hyperspectral curve by its most important structural features first, followed by features of lesser importance.

For an isolated feature, we develop a scale/area relationship: the scale at which its corresponding arch closes is proportional to the cube root of the area enclosed within the feature. Here the area enclosed within the feature refers to the area between the graph of f and the straight line segment connecting the inflection points that delimit the feature. The fingerprint is independent of measuring units chosen for the input function f , although the choice of units does affect the constant of proportionality of the scale/area relationship. Moreover, the fingerprint is unchanged if a linear function is added to f , so that superposition of terrain on a tilted plane leaves the terrain fingerprint unchanged.

Three methods of data extension are compared: (i) end point value extension, (ii) average value extension, and (iii) linear fit to the final five data points at each end of the elevation profile. We argue that extension by linear fit is more appropriate for fingerprint

analysis, since only this method does not introduce spurious inflection points. For numerical convolution with a Gaussian mask, the mask must be cropped to a finite width. The mask size should change dynamically with the standard deviation σ of the Gaussian mask, and should be no less than 3σ in halfwidth. Mask cropping is shown to affect the fingerprint by causing a drift in the location of inflection points at very small σ , especially where the input curve is locally linear. As a consequence we choose to locate the left and right inflection points of features at their 2σ positions.

2. M. A. Piech. Comments on fingerprints of two dimensional edge models. *Computer Vision, Graphics and Image Processing* **42** (1988), 381–386.

Scale space images and fingerprints of the most common two dimensional edge models (step edge, pulse edge and staircase edges) can readily be deduced geometrically from fingerprints of the corresponding one dimensional edge models.

At smoothing scale σ , the range of influence of a feature edge is approximately 3σ units. A practical consequence of this 3σ effect is that fingerprints of adjacent edges will be identical to those of individual isolated edges up to a scale of one-third the distance between the edges.

3. M. A. Piech and K. R. Piech. Hyperspectral interactions: invariance and scaling. *Applied Optics* **28** (1989), 481–489.

Dominant scale space features (i.e. pairings of inflection points that persist over large smoothing scale ranges) can be used to segment a profile into independent regions. The strength and location of features in one region (as measured by fingerprint analysis) are independent of features in other regions. Consequently, fingerprint analysis can be carried out on the individual profile regions, and results compared across the regions.

We extend our previous work [1] relating scale to feature area. The scale at which a fingerprint feature vanishes is independent of feature shape, and depends only on the

area of the feature. Scaling and invariance rules are developed for common cases of interacting features. At large feature separations the fingerprint behavior of one feature is independent of the other feature. At smaller separations two features interact and their scales are damped. Below a critical separation distance features nest, and a plot of feature scales from large to small separations exhibits a bifurcation behavior. Scales of features above the bifurcation point, scales of the nested features, and the location of the bifurcation point depend only on feature areas and not on individual feature shape nor on shape-associated parameters.

Terrain modeling results

During the second phase of this program we correlated fingerprint and fractal analysis of elevation profiles from Digital Elevation Model data. The principal results are discussed in publication 4.

4. M. A. Piech and K. R. Piech. Fingerprints and fractal terrain. *Mathematical Geology* 22 (1990), 457–485.

In this paper we describe the application of fingerprint techniques to elevation data for three major landforms: arid shale, humid shale, and granite (Fig. 2). Granite data is drawn from classic examples of fault block mountains in the Sierra Nevada range of California, and from the Sawtooth mountains of central Idaho, which were formed by deep and extensive erosion of the Idaho Batholith. This selection enables us to analyze not only gross distinctions such as those between granite and shale, but also finer distinctions between arid and humid shale, and between granites of different geophysical origins.

The simplest characterization of topographic features from the scale space fingerprint is the feature density function $N(\sigma)$, which represents the number of terrain features that persist beyond a smoothing scale σ (Fig. 3). The feature density function

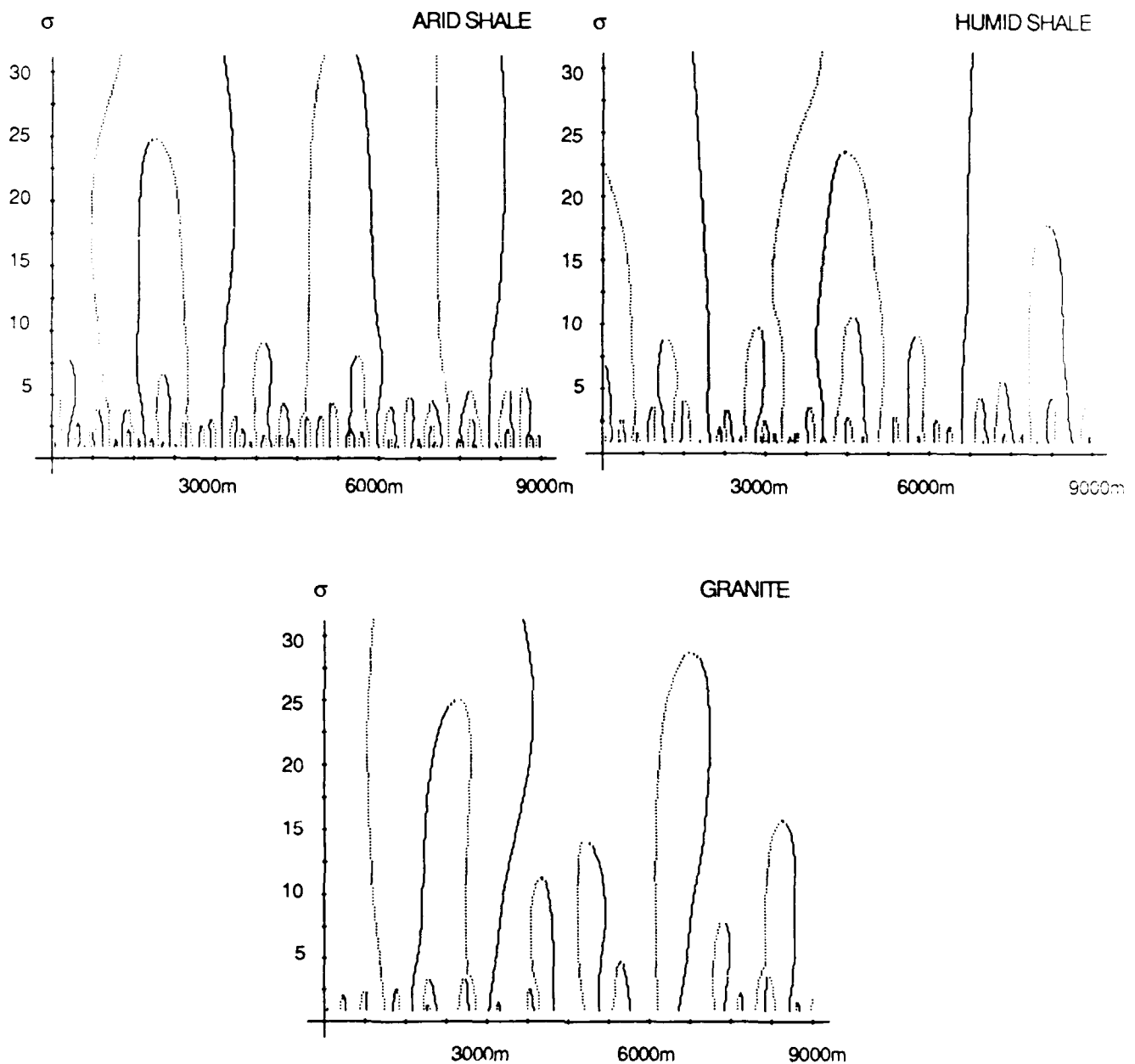


Fig. 2 Typical arid shale, humid shale, and granite fingerprints. The fingerprint features (arches) of arid shale are densely packed with pattern uniformity at small values of σ . Fingerprint features of humid shale are not as densely packed as arid shale (85% as many features as arid shale), and lack pattern uniformity at small scales. The feature density of granite fingerprints is roughly half that of either arid or humid shale, and feature spacing is uneven at most scales.

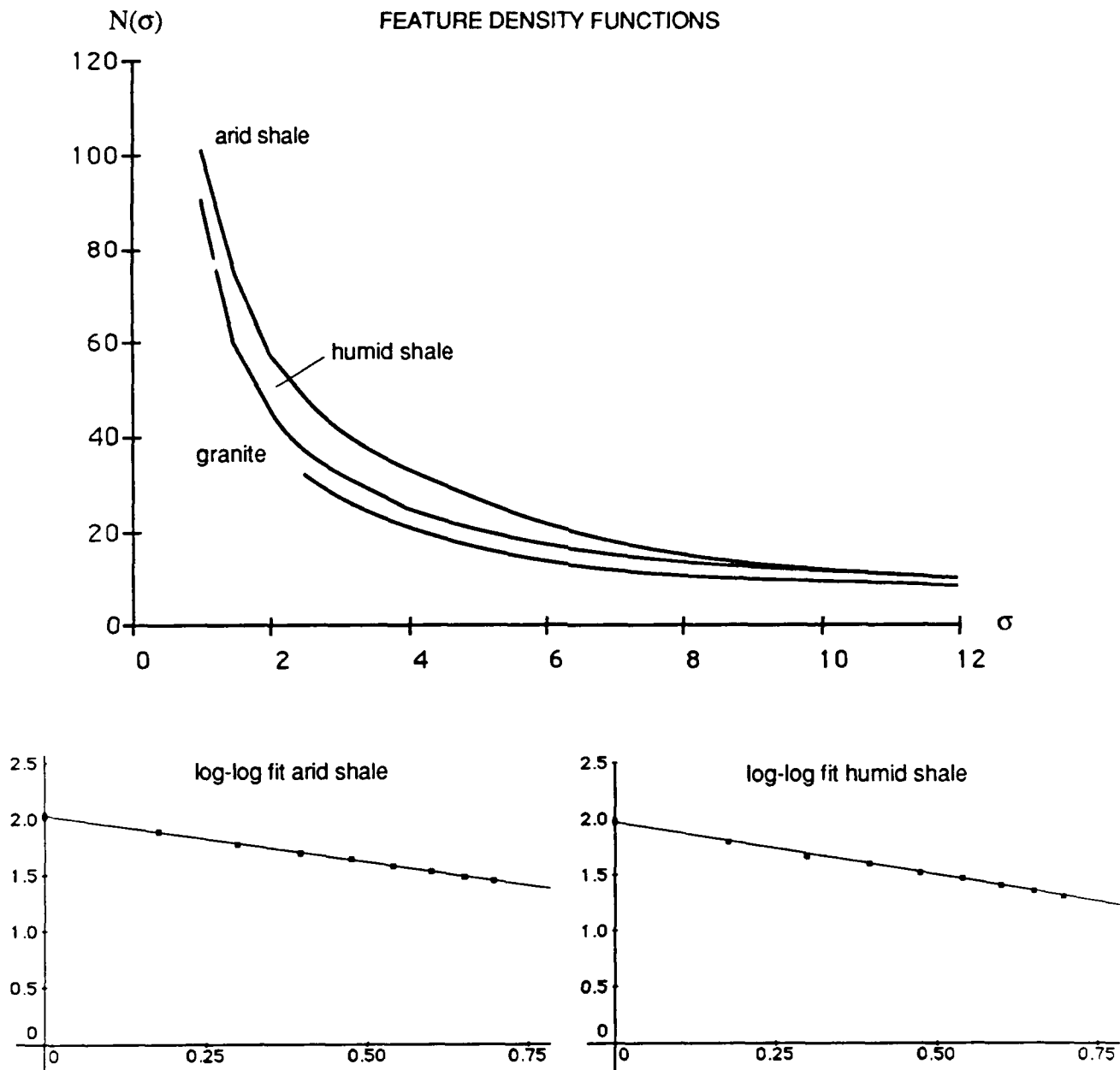


Fig. 3 (Above) Feature density functions, extracted by fingerprint analysis, for arid shale, humid shale, and granite. The granite feature density function is drawn for $\sigma \geq 2.5$, since on this domain CA granite and ID granite have a common feature density function.

(Below) Fractal scaling of the feature density functions for arid and humid shale is confirmed by the log-log linearity of the feature density functions over the range $\sigma = 1$ to 5.

differs for shale and granite landforms and between individual expressions of the landforms such as arid and humid shales. For $\sigma \leq 7$ the feature density functions of granite, arid shale and humid shale are clearly ordered, with $N(\sigma)_{\text{granite}} < N(\sigma)_{\text{humid shale}} < N(\sigma)_{\text{arid shale}}$. Further, the $[N(1), N(1.5)]$ pair of the feature density function is a strong discriminant between shale and granite, between arid and humid shale, and between CA and ID granites. The ordering of the feature density functions and the number of features at small σ agree with intuitive physical concepts of the prevalence of edges in the topography.

There is an intuitive and natural correspondence between the scale changes used to establish fractal behavior and the scale space smoothing in fingerprint analysis. Both concepts evaluate changes in behavior as a function of measuring or smoothing scale. We therefore attempted to evaluate fractal behavior of the landforms by examining the scale space fingerprints and, in particular, the feature density functions extracted from the fingerprints.

We first applied conventional methods of fractal analysis to determine if the landforms could be described by fractal parameters over a range of physical scales. The conventional methods included computation of trail length and surface area as a function of measuring scale. Both the length and area computations demonstrated that the shales were fractal and the granites were not fractal. However, these conventional methods were surprisingly insensitive to fractal behavior and required careful treatment of the dimensions of coordinates for a meaningful description of fractal behavior.

The fingerprint modeling results in a new expression of fractal scaling from the feature density function. There is strong consistency between the expression of scaling from the feature density function and expressions of scaling by fractal parameters extracted with conventional methods such as area scaling and trail length scaling. The conventional methods and the feature density expression agree in predicting a lack of fractal behavior for granite landforms and in predicting fractal behavior for shale landforms. The feature density expression also agrees quantitatively with the conventional methods for the range of scaling behavior of the shale landforms. The conventional computations

of scaling behavior result in scaling for measuring yardsticks up to 180m for both arid and humid shale. The feature density function exhibits scaling behavior to a σ of 5 units, or 150m. Although we cannot equate a measuring scale with a smoothing scale, because the smoothing scale represents a standard deviation, these scaling ranges are compatible. The fingerprint approach is also much more sensitive to fractal scaling than conventional methods, and automatically provides consistency in scaling units, avoiding difficulties encountered in conventional methods.

Extension of fingerprint theory

Scale space fingerprint theory, as employed in this project, operates on one-dimensional elevation profiles. Although the analysis is quite stable for contiguous profiles, it would be very useful if we could develop a fully two-dimensional (2-D) fingerprint theory which would enable tracking from coarse to fine scales in order to accurately locate feature boundaries. Toward the end of this project we studied 2-D edge detection theories to determine whether current theories could serve as a basis for a fingerprint theory. Publication 5 follows from these studies.

5. M. A. Piech. Decomposing the Laplacian. *Pattern Analysis and Machine Intelligence*, to appear.

In a recent paper on authenticating edges detected by zero-crossings of second order differential operators, Clark [Ref.1] derived a formula which shows that the Laplacian $\nabla^2 f$ differs from the second directional derivative $\frac{\partial^2 f}{\partial n^2}$ in the gradient direction of f by the product of the curvature κ of the level curve for f through (x, y) with the gradient magnitude $|\nabla f|$. In this note we present an elementary proof of Clark's formula.

We believe that an entirely new approach to 2-D feature detection, based on the tracking of curvature regions with increased Gaussian filtering, can serve as a basis for a

truly two-dimensional scale space fingerprint theory. We have been exploring the behavior of zero curves of the Gaussian curvature, as the surface undergoes progressive smoothing. The graph of these zero curves versus smoothing scale resembles a glove, and we would hope to eventually be able to characterize terrain type by feature density functions (drawn from the glove) which enumerate the areal density of features as a function of their persistence across smoothing scales. Such a 2-D fingerprint theory would be a more appropriate and valuable descriptor for terrains.

References

1. J. J. Clark, "Authenticating edges produced by zero-crossing algorithms," *IEEE Trans. Pattern Anal. Mach. Intell.* **11** (1989), 43-57.
2. A. P. Witkin, "Scale-space filtering," in *Proceedings, International Joint Conference Artificial Intelligence*, Karlsruhe (1983).
3. A. L. Yuille and T. Poggio, "Fingerprints theorems for zero crossings," *J. Optical Soc. of America A* **2** (1985), 683-692.

IV. Publications

1. M. A. Piech and K. R. Piech. Symbolic representation of hyperspectral data. *Applied Optics* **26** (1987), 4018-4026.
2. M. A. Piech. Comments on fingerprints of two dimensional edge models. *Computer Vision, Graphics and Image Processing* **42** (1988), 381-386.
3. M. A. Piech and K. R. Piech. Hyperspectral interactions: invariance and scaling. *Applied Optics* **28** (1989), 481-489.
4. M. A. Piech and K. R. Piech. Fingerprints and fractal terrain. *Mathematical Geology* **22** (1990), 457-485.
5. M. A. Piech. Decomposing the Laplacian. *Pattern Analysis and Machine Intelligence*, to appear.

V. Abstracts of Publications Listed Above

Symbolic Representation of Hyperspectral Data

We develop a symbolic representation of hyperspectral data using the scale space techniques of Witkin. We create a scale space image of hyperspectral data from convolution with Gaussian masks and then a 'fingerprint' that extracts individual features from the original data. The fingerprint provides a context that pairs inflection points and assigns them to a feature; generates a measure of importance for each feature; and relates features to each other. The representation is an ordered sequence of triplets containing: a measure of importance related to the area of each feature, and the left and right inflection points of the feature. The description is compact, quantitative and hierarchical, describing the hyperspectral curve by its most important structural features first, followed by features of lesser importance.

Comments on Fingerprints of Two Dimensional Edge Models

Shah, Sood and Jain have recently published an interesting scale space analysis of pulse and staircase edge models, both one and two dimensional. In this note we comment upon Shah, Sood and Jain's analysis of the two dimensional step edge, pulse edge and staircase edge models. Their derivation of the scale space images and fingerprints can be simplified by taking advantage of a key geometric feature of Gaussian filters, namely, rotational invariance. The fingerprints of these three models can easily and directly be geometrically deduced from the fingerprints of the one dimensional models. The fingerprints should be viewed as cylinders over a base curve which is precisely the fingerprint of the corresponding one dimensional edge model. In this way fingerprints of the two dimensional models can be immediately visualized from their one dimensional counterparts. We also demonstrate that the range of influence of one edge upon another edge located a distance d away begins at a scale of $d/3$.

Hyperspectral Interactions: Invariance and Scaling

We present new invariance and scaling results for scale space analysis of hyperspectral data. First, we note that a hyperspectral curve can be segmented into independent regions selected by features of scale space fingerprints. These fingerprint features are persistent inflection points that

precisely locate major atmospheric features that define the regions. The strength and location of hyperspectral features in one atmospheric region are independent of features in other regions; as a result, hyperspectral analysis can be simplified to a region-by-region analysis. We then generate simple scaling and invariance rules for features within such a spectral region. We show that the scale of individual features is independent of the details of feature shape and depends only on the area of the feature. Interacting features in turn exhibit a fascinating bifurcation behavior: at large separations features behave independently; at smaller separations features interact and their scales are damped; below a critical separation distance (the bifurcation point) the features nest. The scales of features above the bifurcation point, the scales of the nested features, and the location of the bifurcation point depend only on the feature areas and not on shape-associated parameters of the individual features.

Fingerprints and Fractal Terrain

Scale space fingerprints provide a natural formalism for modeling terrains because they describe a hierarchy of edges over a broad range of physical scales. The simplest fingerprint descriptor is the feature density function $N(\sigma)$ —the number of terrain edges remaining after smoothing a terrain profile with a gaussian of standard deviation σ . Feature density functions computed from Digital Elevation Model data are not only clearly different for landforms such as shales and granite, but also for landform expressions such as arid and humid shale.

Feature density also provides a description of fractal behavior that agrees with conventional fractal computations such as area and trail length scaling; shales exhibit fractal behavior over scales up to about 200 meters, while granites are not fractal over any meaningful range. The feature density evaluation of fractal behavior, however, is superior to the conventional methods: it is more sensitive to the expression of fractal scaling and does not exhibit a dependence on measuring units that can mask fractal behavior in the conventional methods.

Decomposing the Laplacian

We correct and give an elementary derivation of Clark's decomposition of the Laplacian $\nabla^2 f(x,y)$ into a second directional derivative in the gradient direction of f , and a product of gradient magnitude by curvature of the level curve through $f(x,y)$.

VI. Participating Scientific Personnel

M. Ann Piech

Professor of Mathematics, University at Buffalo. Principal Investigator for this project.

Kenneth R. Piech

President, Aspen Analytics. Consultant on this project.

Yu-Tai Huang

Graduate Assistant. PhD dissertation will be on 2-D scale space theory.

Y-H Chang, S-G Chen

Graduate Assistants. Assisted with computing.

Debra Luczkiewicz, Gerard Lanois

Computer programmers. Developed and programmed algorithms.

UNCLASSIFIED

SECURITY CLASSIFICATION OF THIS PAGE (When Data Entered)

REPORT DOCUMENTATION PAGE		READ INSTRUCTIONS BEFORE COMPLETING FORM
1. REPORT NUMBER <i>ARO 23815.6-65</i>	2. GOVT ACCESSION NO. N/A	3. RECIPIENT'S CATALOG NUMBER N/A
4. TITLE (and Subtitle) FRACTAL TERRAIN ANALYSIS FROM AN ATTRACTOR VIEWPOINT		5. TYPE OF REPORT & PERIOD COVERED FINAL REPORT 7/15/86 to 12/31/89
		6. PERFORMING ORG. REPORT NUMBER
7. AUTHOR(s) M. Ann Piech		8. CONTRACT OR GRANT NUMBER(s) DAAL03-86-K-0141
9. PERFORMING ORGANIZATION NAME AND ADDRESS Research Foundation of State University of New York, P.O. Box 9, Albany NY 12201		10. PROGRAM ELEMENT, PROJECT, TASK AREA & WORK UNIT NUMBERS
11. CONTROLLING OFFICE NAME AND ADDRESS U. S. Army Research Office Post Office Box 12211 Research Triangle Park, NC 27709		12. REPORT DATE 2/26/90
14. MONITORING AGENCY NAME & ADDRESS (if different from Controlling Office)		13. NUMBER OF PAGES 18
		15. SECURITY CLASS. (of this report) Unclassified
		15a. DECLASSIFICATION/DOWNGRADING SCHEDULE
16. DISTRIBUTION STATEMENT (of this Report) Approved for public release; distribution unlimited.		
17. DISTRIBUTION STATEMENT (of the abstract entered in Block 20, if different from Report) NA		
18. SUPPLEMENTARY NOTES The view, opinions, and/or findings contained in this report are those of the author(s) and should not be construed as an official Department of the Army position, policy, or decision, unless so designated by other documentation.		
19. KEY WORDS (Continue on reverse side if necessary and identify by block number) scale space fingerprint, terrain model, maps, maps, feature extraction, landform, fractal, maps, R. 2, 3, 4, 5, 6, 7, 8, 9, 10, 11, 12, 13, 14, 15, 16, 17, 18, 19, 20, 21, 22, 23, 24, 25, 26, 27, 28, 29, 30, 31, 32, 33, 34, 35, 36, 37, 38, 39, 40, 41, 42, 43, 44, 45, 46, 47, 48, 49, 50, 51, 52, 53, 54, 55, 56, 57, 58, 59, 60, 61, 62, 63, 64, 65, 66, 67, 68, 69, 70, 71, 72, 73, 74, 75, 76, 77, 78, 79, 80, 81, 82, 83, 84, 85, 86, 87, 88, 89, 90, 91, 92, 93, 94, 95, 96, 97, 98, 99, 100, 101, 102, 103, 104, 105, 106, 107, 108, 109, 110, 111, 112, 113, 114, 115, 116, 117, 118, 119, 120, 121, 122, 123, 124, 125, 126, 127, 128, 129, 130, 131, 132, 133, 134, 135, 136, 137, 138, 139, 140, 141, 142, 143, 144, 145, 146, 147, 148, 149, 150, 151, 152, 153, 154, 155, 156, 157, 158, 159, 160, 161, 162, 163, 164, 165, 166, 167, 168, 169, 170, 171, 172, 173, 174, 175, 176, 177, 178, 179, 180, 181, 182, 183, 184, 185, 186, 187, 188, 189, 190, 191, 192, 193, 194, 195, 196, 197, 198, 199, 200, 201, 202, 203, 204, 205, 206, 207, 208, 209, 210, 211, 212, 213, 214, 215, 216, 217, 218, 219, 220, 221, 222, 223, 224, 225, 226, 227, 228, 229, 230, 231, 232, 233, 234, 235, 236, 237, 238, 239, 240, 241, 242, 243, 244, 245, 246, 247, 248, 249, 250, 251, 252, 253, 254, 255, 256, 257, 258, 259, 260, 261, 262, 263, 264, 265, 266, 267, 268, 269, 270, 271, 272, 273, 274, 275, 276, 277, 278, 279, 280, 281, 282, 283, 284, 285, 286, 287, 288, 289, 290, 291, 292, 293, 294, 295, 296, 297, 298, 299, 300, 301, 302, 303, 304, 305, 306, 307, 308, 309, 310, 311, 312, 313, 314, 315, 316, 317, 318, 319, 320, 321, 322, 323, 324, 325, 326, 327, 328, 329, 330, 331, 332, 333, 334, 335, 336, 337, 338, 339, 340, 341, 342, 343, 344, 345, 346, 347, 348, 349, 350, 351, 352, 353, 354, 355, 356, 357, 358, 359, 360, 361, 362, 363, 364, 365, 366, 367, 368, 369, 370, 371, 372, 373, 374, 375, 376, 377, 378, 379, 380, 381, 382, 383, 384, 385, 386, 387, 388, 389, 390, 391, 392, 393, 394, 395, 396, 397, 398, 399, 400, 401, 402, 403, 404, 405, 406, 407, 408, 409, 410, 411, 412, 413, 414, 415, 416, 417, 418, 419, 420, 421, 422, 423, 424, 425, 426, 427, 428, 429, 430, 431, 432, 433, 434, 435, 436, 437, 438, 439, 440, 441, 442, 443, 444, 445, 446, 447, 448, 449, 450, 451, 452, 453, 454, 455, 456, 457, 458, 459, 460, 461, 462, 463, 464, 465, 466, 467, 468, 469, 470, 471, 472, 473, 474, 475, 476, 477, 478, 479, 480, 481, 482, 483, 484, 485, 486, 487, 488, 489, 490, 491, 492, 493, 494, 495, 496, 497, 498, 499, 500, 501, 502, 503, 504, 505, 506, 507, 508, 509, 510, 511, 512, 513, 514, 515, 516, 517, 518, 519, 520, 521, 522, 523, 524, 525, 526, 527, 528, 529, 530, 531, 532, 533, 534, 535, 536, 537, 538, 539, 540, 541, 542, 543, 544, 545, 546, 547, 548, 549, 550, 551, 552, 553, 554, 555, 556, 557, 558, 559, 560, 561, 562, 563, 564, 565, 566, 567, 568, 569, 570, 571, 572, 573, 574, 575, 576, 577, 578, 579, 580, 581, 582, 583, 584, 585, 586, 587, 588, 589, 590, 591, 592, 593, 594, 595, 596, 597, 598, 599, 600, 601, 602, 603, 604, 605, 606, 607, 608, 609, 610, 611, 612, 613, 614, 615, 616, 617, 618, 619, 620, 621, 622, 623, 624, 625, 626, 627, 628, 629, 630, 631, 632, 633, 634, 635, 636, 637, 638, 639, 640, 641, 642, 643, 644, 645, 646, 647, 648, 649, 650, 651, 652, 653, 654, 655, 656, 657, 658, 659, 660, 661, 662, 663, 664, 665, 666, 667, 668, 669, 670, 671, 672, 673, 674, 675, 676, 677, 678, 679, 680, 681, 682, 683, 684, 685, 686, 687, 688, 689, 690, 691, 692, 693, 694, 695, 696, 697, 698, 699, 700, 701, 702, 703, 704, 705, 706, 707, 708, 709, 710, 711, 712, 713, 714, 715, 716, 717, 718, 719, 720, 721, 722, 723, 724, 725, 726, 727, 728, 729, 730, 731, 732, 733, 734, 735, 736, 737, 738, 739, 740, 741, 742, 743, 744, 745, 746, 747, 748, 749, 750, 751, 752, 753, 754, 755, 756, 757, 758, 759, 760, 761, 762, 763, 764, 765, 766, 767, 768, 769, 770, 771, 772, 773, 774, 775, 776, 777, 778, 779, 780, 781, 782, 783, 784, 785, 786, 787, 788, 789, 790, 791, 792, 793, 794, 795, 796, 797, 798, 799, 800, 801, 802, 803, 804, 805, 806, 807, 808, 809, 810, 811, 812, 813, 814, 815, 816, 817, 818, 819, 820, 821, 822, 823, 824, 825, 826, 827, 828, 829, 830, 831, 832, 833, 834, 835, 836, 837, 838, 839, 840, 841, 842, 843, 844, 845, 846, 847, 848, 849, 850, 851, 852, 853, 854, 855, 856, 857, 858, 859, 860, 861, 862, 863, 864, 865, 866, 867, 868, 869, 870, 871, 872, 873, 874, 875, 876, 877, 878, 879, 880, 881, 882, 883, 884, 885, 886, 887, 888, 889, 890, 891, 892, 893, 894, 895, 896, 897, 898, 899, 900, 901, 902, 903, 904, 905, 906, 907, 908, 909, 910, 911, 912, 913, 914, 915, 916, 917, 918, 919, 920, 921, 922, 923, 924, 925, 926, 927, 928, 929, 930, 931, 932, 933, 934, 935, 936, 937, 938, 939, 940, 941, 942, 943, 944, 945, 946, 947, 948, 949, 950, 951, 952, 953, 954, 955, 956, 957, 958, 959, 960, 961, 962, 963, 964, 965, 966, 967, 968, 969, 970, 971, 972, 973, 974, 975, 976, 977, 978, 979, 980, 981, 982, 983, 984, 985, 986, 987, 988, 989, 990, 991, 992, 993, 994, 995, 996, 997, 998, 999, 1000		

20 continued

order of importance based on edge strength, they provide a natural approach for terrain analysis. Therefore, we applied scale space fingerprints as a primary analysis tool to Digital Elevation Models of various terrain types. Scale space fingerprint analysis yields two important results for terrain modeling: First, by using a feature density function that describes the number of terrain edges as a function of smoothing scale, we were able to discriminate between different landforms and even between different expressions of the same landform. And, using the same feature density function as a descriptor, we were able to determine fractal behavior of a landform more sensitively than by conventional methods, and without a dependence on measuring units that can mask fractal behavior. We also initiated theory development for a two dimensional fingerprint capability based on the gaussian curvature operator,

20 continued
2010-01-01